Cell Stress & Chaperones (2005) **10** (3), 171–184

Article no. csac. 2005.CSC-107R

Differential expression of alphaB-crystallin and Hsp27-1 in anaplastic thyroid carcinomas because of tumor-specific alphaB-crystallin gene (CRYAB) silencing

Ivelina Mineva,[1] Wolfgang Gartner,[1] Peter Hauser,[1] Alexander Kainz,[1] Michael Löffler,[1] Gerhard Wolf,[2] Rainer Oberbauer,[1] Michael Weissel,[1] and Ludwig Wagner[1]

[1]Department of Medicine III, Medical University of Vienna, Waehringer Guertel 18-20, Vienna A-1090, Austria
[2]Department of Surgery, Medical University of Graz, Graz, Austria

Abstract Expression of the small heat shock protein alphaB-crystallin in differentiated thyroid tumors has been described recently. In this study, we investigated the molecular mechanisms that affect the expression of alphaB-crystallin in benign goiters ($n = 7$) and highly malignant anaplastic thyroid carcinomas (ATCs) ($n = 3$). AlphaB-crystallin expression was compared with that of Hsp27-1. Immunoblot and quantitative real-time (RT) polymerase chain reaction revealed marked downregulation of alphaB-crystallin in all the tested ATCs and the ATC-derived cell line C-643 . In contrast, considerable expression of Hsp27-1 in benign and malignant thyroid tissue was demonstrated. Immunofluorescence analysis revealed no relevant topological differences between benign and malignant thyrocytes in the cytoplasmic staining of both proteins. Consistent and marked downregulation of TFCP2L1 was identified as one of the main mechanisms contributing to CRYAB gene silencing in ATCs. In addition, CRYAB gene promoter methylation seems to occur in distinct ATCs. In silico analysis revealed that the differential expression of alphaB-crystallin and Hsp27-1 results from differences between the alphaB-crystallin and Hsp27-1 promoter fragments (712 bp upstream from the transcriptional start site). Biological activity of the analyzed promoter element is confirmed by its heat shock inducibility. In conclusion, we demonstrate downregulation of alphaB-crystallin expression in highly dedifferentiated ATCs because of a tumor-specific transcription factor pattern. The differential expression of alphaB-crystallin and Hsp27-1 indicates functional differences between both proteins.

INTRODUCTION

Small heat shock proteins represent a large protein family with a molecular weight of 15–30 kDa. The important biological function of small heat shock proteins is reflected by conservation of their structure from bacteria to humans. In mammals, 10 different small heat shock proteins have been identified, eg, alphaB-crystallin and Hsp27-1 (Kappe et al 2001, 2003). Because of heat shock factor responsive elements within their promoter regions, alphaB-crystallin and Hsp27-1 are heat-inducible proteins (Hickey et al 1986; Dubin et al 1990). AlphaB-crystallin and Hsp27-1, which exhibit sequence and functional similarity (Mehlen et al 1996), were experimentally induced in the presence of various types of cellular stress including thermal shock (Muchowski et al 1999), osmotic shock (Dasgupta et al 1992), oxidative insults, ischemia, (Bluhm et al 1998; Golenhofen et al 1998), or exposure to heavy metals. Both proteins have been shown to protect from cellular stress by several mechanisms. They facilitate renaturation of denatured proteins (Derham and Harding 1999) and protect cytoskeletal elements from ischemic injury and aggregation (Liang and MacRae 1997; Mitton et al 1997; Kamradt et al 2001; Parcellier et al 2005). AlphaB-crystallin stabilizes actin filaments and decreases actin depolymerization (Wang and Spector 1996). It is estab-

Correspondence to: Ludwig Wagner, Tel: 43-1-40400/4341; Fax: 43-1-40400/7790; E-mail: ludwig.wagner@meduniwien.ac.at.
Received 14 January 2005; Revised 1 March 2005; Accepted 3 March 2005.

lished that small heat shock proteins such as alphaB-crystallin and Hsp27-1 inhibit apoptosis (Mehlen et al 1996; Garrido et al 2001, 2003; Kamradt et al 2001; Webster 2003). In this context, it is of interest that alphaB-crystallin has been shown to promote muscle cell survival during myocyte differentiation (Kamradt et al 2002).

Small heat shock proteins are widely distributed in mammalian tissues. For example, alphaB-crystallin is one of the structural proteins of the eye lens, where it takes part in maintaining transparency (Groenen et al 1994; Horwitz 2003). In addition, alphaB-crystallin is expressed in many nonlenticular tissues including heart, brain, skeletal muscles, skin, lung, and to a lower extent in the kidney and thyroid gland (Dubin et al 1989; Iwaki et al 1990; Klemenz et al 1993). AlphaB-crystallin expression has also been demonstrated to varying extent in numerous epithelial tumors (Pinder et al 1994). Similarly, Hsp27-1 expression was found in various benign and malignant tissues, eg, in retinal neurons (Whitlock et al 2005a, 2005b), in reproductive tissues (White et al 2005), in normal and neoplastic renal tissue (Neuhofer et al 2005; Tremolada et al 2005), and in malignant thyroid tissue (Akslen and Varhaug 1995).

We recently reported differential heat shock protein expression in benign and malignant endocrine tissues (Zierhut et al 2004). On the basis of these findings and motivated by the fact that alphaB-crystallin expression has been demonstrated in differentiated thyroid tumors, we investigated the expression of alphaB-crystallin in benign thyroid tissue and in highly malignant anaplastic thyrocytes and compared it with the expression of Hsp27-1. Consistent downregulation of alphaB-crystallin in anaplastic thyroid carcinoma (ATC)–derived tissue is demonstrated. As the main underlying cause, a tumor-characteristic transcription factor pattern characterized by marked downregulation of the CRYAB gene promoter–interacting transcription factor TFCP2L1 was identified.

MATERIALS AND METHODS

Reagents

The anti–αB-crystallin antibody (catalog no. 2387029) was obtained from Calbiochem (Darmstadt, Germany), and anti–Hsp27-1 monoclonal antibody (mAb) (catalog no. H1830-51) was purchased from US Biological (Swampscott, MA, USA). The anti-actin antibody (catalog no. A2066) was obtained from Sigma (Vienna, Austria). The Alexa Fluor 488 $F(ab')_2$ goat anti-rabbit immunoglobulin (Ig) (catalog no. A-11034) is available at Invitrogen (San Diego, CA, USA), AffiniPure $F(ab')_2$ goat anti-mouse Ig (catalog no. JGM026062) was obtained from Accurate Chemical & Scientific Corporation (Westbury, NY, USA). TITANIUM One-Step RT-polymerase chain reaction (PCR) Kit was obtained from Clontech (Palo Alto, CA, USA). S-Gal™/Luria-Bertani (LB) Agar (C-4478), Triton X-100, aprotinin, pepstatin, leupeptin, Pefabloc, ampicillin, diethylpyrocarbonate (DEPC) treated water, and ethidium bromide are Sigma reagents. Kodak XAR5-Omat films are Sigma reagents (St Louis, MO, USA). BamH1, EcoR1, Boehringer Mannheim chemoluminescence blotting substrate, T4 deoxyribonucleic acid (DNA) ligase, and TRIzol® reagent were obtained from Roche Diagnostics (Mannheim, Germany). Molecular weight markers (DNA III) were purchased from Boehringer Mannheim (Vienna, Austria). Gatewate LR Clonase Enzyme mix, One Shot™ cells (INVαF′), pENTR Directional TOPO Cloning Kit, pDEST15 were obtained from Invitrogen. Peroxidase-conjugated goat anti-rabbit Ig was obtained from DAKO (Glostrup, Denmark). Plasmid Purification Kits are from QIAGEN (Hilden, Germany). SOC medium was purchased from GIBCO-BRL Life technologies (Paisley, Scotland). The pGEM-T Easy Vector System I was from Promega (Madison, WI, USA). The Bicinchoninic Acid (BCA) Protein assay kit was purchased from PIERCE (Rockford, IL, USA). Klenow enzyme, Northern Max Low and High Stringency Wash Solution; ULTRAhyb hybridization buffer—Ambion (Austin, TX, USA), and ^{32}P-deoxycytidine 5′-triphosphate (dCTP) was obtained from Amersham Pharmacia Biotech (Uppsala, Sweden).

Immunofluorescence

Cryosections (4 μm) were fixed in acetone for 5 minutes and incubated with the anti–alphaB-crystallin rabbit antibody (diluted 1:300 in phosphate-buffered saline [PBS]) or anti–Hsp27-1 mAb (diluted 1:500 in PBS) or with PBS as a negative control for 1 hour, followed by incubation with the Alexa Fluor™ 488 labeled $F(ab')_2$ goat anti-rabbit Ig (diluted 1:200) or the TRITC-labeled AffiniPure $F(ab')_2$ goat anti-mouse Ig, respectively, for 1 hour. All incubation steps were performed in a moist chamber under light protection and were followed by PBS washing steps for 10 minutes. Finally, the slides were mounted with Vectashield (Vector Laboratories, Burlingame, CA, USA) and viewed under a Leica Aristoplan microscope. Images were recorded using Leica Image Manager software and further arranged with Adobe Photoshop software.

To test for Ab specificity, the alphaB-crystallin Ab was preadsorbed with human recombinant alphaB-crystallin. Preadsorption was carried out at a molar ratio of 5:1 (antigen:Ab) at 4°C for 2 hours.

Tissue preparation

Tissues were removed by surgery and immediately snap frozen in liquid nitrogen. Tissue samples were cut into fragments on dry ice, and aliquots were stored in cryo-

tubes in liquid nitrogen. Tissue fragments (~200 mg) were homogenized in 300 μL precooled homogenization buffer (Tris-buffered saline containing 1% Triton X-100, 10 μg/mL aprotinin, 1 μg/mL pepstatin, 10 μg/mL leupeptin, and 0.8 mM Pefabloc). After preclearing the homogenate by centrifugation at 10 000 × *g* for 10 minutes at 4°C, the protein content was measured using the Micro BCA Protein assay kit. Tissue processing was approved by the local ethics committee, and informed consent was obtained from each patient.

Immunoblot analysis

Tissue extract aliquots (12 μg total protein) were loaded onto a 12% sodium dodecyl sulfate–polyacrylamide gel electrophoresis under reducing conditions, followed by electrophoretic transfer to nitrocellulose. The membrane was blocked with 10% skim milk, incubated with a monospecific rabbit polyclonal anti–alphaB-crystallin antibody or anti–Hsp27-1 mAb followed by peroxidase-conjugated goat anti-rabbit or goat anti-mouse Ig, respectively, and further developed by BM chemoluminescent reagent (Roche Molecular Biochemicals, Vienna, Austria). Each incubation step was followed by 2 washing steps in PBS buffer supplemented with 0.1% Tween-20.

Quantitative real-time PCR

Total ribonucleic acid (RNA) was isolated using a Polytron tissue homogenizer and TRIzol™ reagent according to the manufacturer's instructions. Isolated RNA was reverse transcribed after deoxyribonuclease (DNase) I (Invitrogen, Carlsbad, CA, USA) treatment using Superscript II (Invitrogen) and random hexamer primers (Invitrogen) according to the test manual. In brief, 1 μg RNA diluted in 9 μL DNase reaction buffer was incubated with 1 μL DNase I at room temperature for 15 minutes. The reaction was stopped using 1 μL 25 mM ethylenediaminetetraacetic acid followed by incubation at 65°C for 15 minutes. For complementary DNA (cDNA) synthesis, 4 μL of 5× first strand buffer together with 2 μL dithiothreitol, 1 μL deoxynucleoside triphosphate mix (10 mM), 1 μL random primers, and ribonuclease (RNAse) inhibitor with 1 μL SuperScript II were incubated for 10 minutes at 25°C followed by 50 minutes incubation at 42°C. After stopping the reaction by incubation at 70°C for 15 minutes, 80 μL H_2O was added. Real-Time PCR amplifications were performed using gene-specific 6-carboxyfluorescin (FAM)-carboxytetramethyl-rhodamine (TAMRA)–labeled Assay-on-Demand (Applied Biosystems, Forster City, CA, USA) normalized to 18S Vic-TAMRA–labeled endogenous control (Applied Biosystems). Gene-specific messenger RNA (mRNA) was quantitated in duplicates in an ABI PRISM 7000 Cycler (Applied Biosystems).

Reverse transcription–PCR and cDNA cloning of alphaB-crystallin

RNA isolated from tissue samples testing positive for alphaB-crystallin expression at the immunoblot level was subjected to the One-Step reverse transcription-PCR procedure (TITANIUM, BD Biosciences). First strand cDNA synthesis was carried out at 50°C for 1 hour. This was followed by gene-specific PCR amplification. The cycling parameters (30 cycles) were as follows: 94°C (30 seconds) for denaturation, 52°C (30 seconds) for annealing, and 72°C (60 seconds) for synthesis using gene-specific primers (forward: 5′ATGGACATCGCCATCCAC′3, reverse: 5′CTATTTCTTGGGGGCTGC′3). The PCR products were separated on a 1% agarose gel. Positive products (2 μl) were cloned into the pGEM-T Easy vector (1 μL, Promega) using 2× ligation buffer (5 μL), T4 DNA ligase (1 μL), and sterile water (1 μL). The ligation reactions were incubated at room temperature for 1 hour and subsequently transformed into One Shot TOP10 competent cells by the heat shock technique. After blue-white screening, positive testing plasmids were isolated and tested for alphaB-crystallin coding sequence by restriction enzyme digest and sequencing.

Directional cloning of the alphaB-crystallin coding sequence

For directional cloning of the alphaB-crystallin coding sequence into pENTRY/D-TOPO vector, the pGEM-T Easy-alphaB-crystallin insert was used as PCR template and the alphaB-crystallin primer was modified by addition of CACC at the 5′-end of the forward primer. Thermal cycling parameters (25 cycles) were as follows: 94°C (30 second) for denaturation, 55°C (30 second) for annealing, and 72°C (60 seconds) for synthesis. The PCR product (2 μL) was cloned into the pENTRY/D-TOPO vector (1 μL) using the TOPO Cloning Reaction Protocol (1 μL salt solution, 2 μL PCR product, and 3 μL H_2O). After incubation at room temperature for 5 minutes, 1.5 μL ligation reaction was used for transformation of One Shot TOP10 chemically competent *Escherichia coli* (50 μL) using the heat shock method. The transformants were spread onto LB agar plates containing kanamycin (27 μg/mL). Colonies were selected by restriction enzyme digest. Chosen clones were amplified and purified by QIAGEN Plasmid Midi Protocol.

Cloning of mammalian GST-alphaB-crystallin fusion protein

The alphaB-crystallin insert was shifted from pENTRY/D-TOPO vector to glutathione-S transferase (GST) N-ter-

minal fusion vector (pDEST 15, Invitrogen) using Gateway LR Clonase Enzyme Mix (Invitrogen). In brief, pENTRY/D-TOPO-alphaB-crystallin (300 ng) and pDEST 15 (300 ng) were mixed with 4 μL 5× LR Clonase Reaction Buffer (Invitrogen) and RNase-free water to 16 μL, followed by addition of 4 μL of LR Clonase Enzyme Mix (Invitrogen), and a final incubation step for 1 hour at room temperature. One microliter of the reaction was used for transformation of TOP10 competent cells by the heat shock method. Transformants (100 μL) were then spread onto LB agar plates containing 50 μg/mL of ampicillin and incubated at 37°C overnight. Selected colonies were amplified and alphaB-crystallin fusion protein–encoding plasmids were purified by QIAGEN Plasmid Midi Protocol.

DNA isolation and Southern blot analysis

Tumor tissue was homogenized using a Polytron tissue homogeniser (Kinematica, Kriens, Switzerland) or using a tissue grinder and grinding tubes without resin (Amersham Biosciences, San Francisco, CA, USA). DNA was isolated after protease K digestion by the phenol–chloroform–isoamylalcohol method using a standard technique. DNA (20 μg) was incubated with *Taq*1 enzyme (65°C, overnight, constant shaking) and with EcoR1 and BamH1 (37°C, overnight), respectively. The digested DNA was loaded onto a 1.2% agarose gel for electrophoretic separation. The gel was subsequently acidified in 10 gel volumes of 0.25 M HCl for 30 minutes and denatured in 1.5 M NaCl/0.5 M NaOH for 20 minutes. After neutralization of the gel in 1.5 M NaCl-0.5 M Tris/HCl, pH 7.0, the DNA was transferred onto a Hybond-N membrane and fixed by UV cross-linking. Prehybridization of the membrane was followed by hybridization using a ^{32}P-radiolabeled DNA probe and ULTRAhyb hybridization solution (Ambion). After overnight hybridization at 42°C, blots were washed using NorthernMax Low Stringency Wash Solution no. 1 (Ambion), followed by NorthernMax High Stringency Wash Solution no. 2 (Ambion) and exposed for autoradiography to Kodak XAR5-Omat films at −80°C.

Cloning of alphaB-crystallin promoter luciferase reporter vector

The PCR-amplified 712-bp-spanning alphaB-crystallin promoter element was cloned into the linearized pMluc-3 renilla reporter vector (Novagen–Merck, Vienna, Austria). In brief, the PCR product (2 μL) was incubated at 4°C overnight together with the pMluc-3 vector (1 μL) and the T4 DNA ligase (1 μL) supplied with the vector kit (Novagen–Merck). The reaction mixture (2 μL) was then transformed into NovaBlue Singles™ Competent cells (Novagen–Merck) using the heat shock method. The bacteria were spread onto Amp/LB/agar plates. Outgrowing colonies were screened for right orientation of the promoter by miniprep plasmid purification and subsequent restriction enzyme digest (Bam H1). After sequence verification, the alphaB-crystallin promoter plasmid was further amplified and purified using the QIAGEN Midi Protocol.

Mammalian cell transfection

Cos cells and the ATC cell line C-643 were transiently transfected with 1 μg of alphaB-crystallin luciferase reporter plasmid using lipofectin (Invitrogen) according to the manufacturer's instructions. Transfection reactions were performed in 6-cm petri dishes. After a 5-hour incubation step, prewarmed complete culture medium RPMI 1640 supplemented with 10% fetal calf serum with the addition of 100 U/mL penicillin and 100 μg/mL streptomycin) was added. After an additional 16-hour incubation (37°C, 5% CO_2), cells were trypsinated and transferred into 24-multiwell dishes for additional analysis.

Heat shock and hyperglycemic shock

Cos cells transfected with the alphaB-crystallin promoter sequence containing luciferase reporter vector or pMluc-3 sham vector as control were either incubated at 40°C, 5% CO_2 or at 37°C, 5% CO_2 humidified incubator (both Cytoperm Heraeus, Vienna, Austria) for 4 hours. After the heat shock, cells were further grown at 37°C, 5% CO_2 in a humidified incubator for 6 hours. Subsequently, tissue culture supernatant was removed and tested for presence of luciferase activity using the MightyLight Rluc Assay kit (Novagen–Merck) according to the manufacturer's manual. In brief, 15 μL of tissue culture supernatant and 100 μL of MightyLight Rluc Substrate were applied to luminometer-compatible tubes. Ranilla luciferase activity was measured 10 seconds after substrate application using the Berthold luminometer (Berthold Technologies, Bad Wildbad, Germany). Cell viability and number were tested to exclude heat shock artifacts. For hyperglycemic shock, Cos cells were exposed to glucose (44 mM) for 4 hours and compared with control conditions (complete culture media).

C-643 ATC cell exposure to 5-azacytidine

C-643 cells were freshly plated onto 5-cm petri dishes. After 12 hours, C-643 cells were exposed to RPMI 1640 cell culture medium supplemented with Hybri-Max containing 0.5 mM 5-azacytidine. C-643 cells were serially harvested after a 24- and 72-hour incubation period. Tissue culture medium containing 5-azacytidine was exchanged every 24 hours. Cells were harvested into 1 mL

TRIzol using a cell scraper. RNA and protein isolation was performed according to the TRIzol manufacturer's instructions.

Promoter sequencing

For promoter sequence analysis, tumor DNA was used as template and alphaB-crystallin promoter–specific primers (forward: 5′-TGGTCAGCTCCTTCAGCT-3′ and reverse: 5′-TTTCCACACCTCATTTTCTCC-3′) were chosen to amplify the identical promoter fragment ranging 712 bp upstream of the transcription start site. Thermal cycling parameters (25 cycles) were set to 94°C (30 seconds) for denaturation, to 53°C (30 seconds) for annealing, and to 72°C (30 seconds) for synthesis using Expand™ high-fidelity polymerase system (Boehringer Mannheim). After size verification of the PCR products, the promoter was cloned into pGEM-T Easy vector as described above. Multiple alphaB-crystallin promoter–containing inserts were amplified and sequenced for each individual tumor.

CpG island methylation analysis

A total of 15 μg of somatic DNA was digested using the methylation-sensitive restriction enzyme *Hpa*II and in parallel the methylation-insensitive isoschizomer *Msp*I. DNA fragments were size fractionated on a 1.5% agarose gel and blotted onto Hybond-N membranes (Amersham Biosciences), using 10× saline-sodium citrate and a capillary blotting device, after gel acidification, denaturation, and neutralization, as described above for the Southern blot analysis. After UV cross-linking (254 nm, 5 minutes), the blot was prehybridized for 5 hours at 42°C and hybridized in ULTRAhyb hybridization buffer (Ambion) with a ^{32}P-dCTP Klenow-labeled random primed probe (cDNA) specific for the alphaB-crystallin coding part (exons 1–3) and for the CRYAB gene promoter (712 bp), respectively (overnight, 42°C). Blots were washed using NorthernMax Low Stringency Wash Solution no. 1 (45°C), followed by NorthernMax High Stringency Wash Solution no. 2 (50°C), and exposed for autoradiography to Kodak XAR5-Omat films at −80°C.

Bioinformatic analysis of the alphaB-crystallin promoter

To analyze responsive elements present at the alphaB-crystallin (CRYAB) and HSPB1 gene promoters, the corresponding stretch of DNA (transcription start site to −712) of both genes was chosen and submitted for a motif search at http://motif.genome.ad.jp/motif-bin/Srch_Motif_Lib. The cutoff value entered for each TRANSFAC database entry for identification of a responsive element was set to 85.

Gene array analysis

Trizol™ isolated RNA was measured using a Hitachi U-2000 spectrophotometer. RNA quality was checked by denaturing gel electrophoresis, ethidium bromide staining, and subsequent analysis with the Agilent 2100 Bioanalyzer and RNA6000 LabChip® kit (Agilent, Palo Alto, CA, USA). Stratagene universal human RNA (Stratagene, La Jolla, CA, USA) was used as a reference in the hybridization procedure.

cDNA arrays consisting of 41 000 genes with known and unknown function (expressed sequence tags) were obtained from the Stanford University Functional Genomics core facility. All gene array experiments were performed as described previously (Perou et al 2000). Detailed protocols are available at http://genome-www.stanford.edu/. In brief, 100 μg of sample and standard total RNA were labeled with CyScribe cDNA postlabeling kit (Amersham Pharmacia Biotech, Buckinghamshire, UK) in a 2-step procedure.

Samples were loaded on arrays and incubated for 16 hours in a 65°C water bath. After 3 washing steps, fluorescent images of hybridized arrays were obtained by using a GenePix 4000B scanner (Axon Instruments, Union City, CA, USA). Image gridding and calculation of spot intensity were performed with GenePix Pro 4.1 software. The primary data tables and the images files were stored in the Stanford microarray database (http://genome-www4.stanford.edu/MicroArray/SMD/) (Sherlock et al 2001).

RESULTS

Comparative alphaB-crystallin and Hsp27-1 expression analysis in benign goiters and highly malignant ATCs

To compare the expression of alphaB-crystallin and Hsp27-1 in benign and malignant thyroid tissue (ATC, $n = 3$; benign goiter, $n = 7$) and the ATC cell line C-643, immunoblot and quantitative RT-PCR analysis was performed. Using immunoblot analysis, alphaB-crystallin was found in each of the tested benign goiter–derived tissues to a similar extent (Fig 1A, lanes 1–7—goiters 1–7). In contrast, alphaB-crystallin was absent (ATC 1 and ATC 2) or markedly downregulated (ATC 3) in ATC-derived tissues (Fig 1A, lanes 8–10—ATCs 1–3). Hsp27-1 was highly and equally expressed in benign and malignant thyroid tissues (Fig 1A, lanes 1–10). Interestingly, the ATC-derived cell line C-643 exhibited loss of both, alphaB-crystallin and Hsp27-1 expression (Fig 1A, lane 11). Loading of comparable protein quantities (~12 μg) was confirmed by parallel actin immunoblotting. Anti–alphaB-crystallin antibody specificity was confirmed by preadsorption with recombinantly expressed alphaB-crystallin, which resulted in complete loss of the immunosignals.

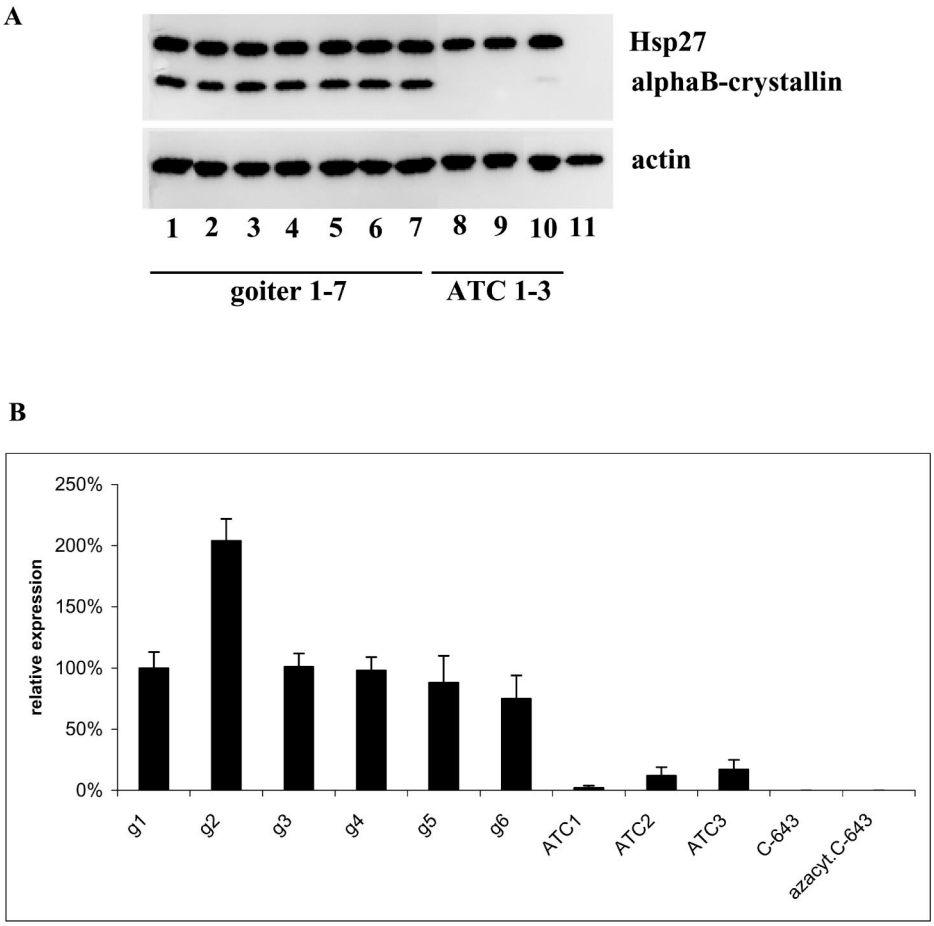

Fig 1. Comparative immunoblot and quantitative RT-PCR analysis of alphaB-crystallin and Hsp27-1 expression in benign goiters and anaplastic thyroid carcinomas (ATCs). (A) Tissue lysate aliquots (~12 μg total protein) derived from goiter and ATC were subjected to 12% polyacrylamide gel electrophoresis and subsequent immunoblotting for alphaB-crystallin and Hsp27-1, respectively. AlphaB-crystallin was considerably and equally expressed in goiters (goiter 1–7, lanes 1–7). In contrast, only missing (ATC 1 and ATC 2, lanes 8 and 9) to marginal (ATC 3, lane 10) alphaB-crystallin immunosignals were detected when ATC-derived tissues were subject of testing. Hsp27-1 was consistently expressed in all the tested thyroid tissue samples (lanes 1–10). The ATC-derived cell line C-643 exhibited neither alphaB-crystallin nor Hsp27-1 specific immunosignals. Loading of comparable protein quantities was confirmed by parallel actin immunoblotting. Shown is 1 representative experiment out of 5. (B) Immunoblot results were verified and quantified by RT-PCR. Results are expressed as levels of alphaB-crystallin ribonucleic acid (RNA) relative to the expression of alphaB-crystallin in goiter 1. Experiments were performed in duplicates (mean ± SD is depicted). For calculation of alphaB-crystallin expression in each tumor 18 S messenger RNA (mRNA) expression was used as reference. Whereas considerable alphaB-crystallin encoding mRNA was present in all the goiter tissues (g1–g6), only marginal amounts were detected in ATC tissue (ATC1–ATC3) and in the ATC cell line C-643. Exposure of C-643 cell to 5-azacytidine had no effect on alphaB-crystallin expression.

To confirm and quantify the immunoblot results, quantitative RT-PCR of goiter and ATC-derived total RNA was performed (Fig 1B). As expected, remarkable expression of alphaB-crystallin in goiter-derived tissue specimens (n = 6, goiter 1 = 100%) but only marginal expression in ATC-derived tissue (n = 3) and in C-643 cells was detected.

Comparative immunofluorescence analysis of the intracellular alphaB-crystallin and Hsp27-1 distribution in goiter and ATC tissue

To characterize the intracellular localization of alphaB-crystallin and Hsp27-1 in benign thyrocytes and to investigate tumor-associated changes in the intracellular distribution of both small heat shock proteins, immunofluorescence analysis was performed. Benign goiter–derived tissues exhibited a high intensity of cytoplasmic alphaB-crystallin immunostaining, which accumulated in juxtaposition to the cell nucleus (Fig 2A,B). As expected from the data presented above, alphaB-crystallin immunosignal intensity was markedly reduced when ATC-derived tissues were the subject of testing. Whereas alphaB-crystallin was undetectable in ATC1 (Fig 2C), marginal staining was present in ATC2 and ATC3 (data not shown). Hsp27-1 immunofluorescence was found to a similar extent in goiter-derived (Fig 2D) and ATC-derived (Fig 2E) tissue specimens. Interestingly, ATC1 (Fig 2E)

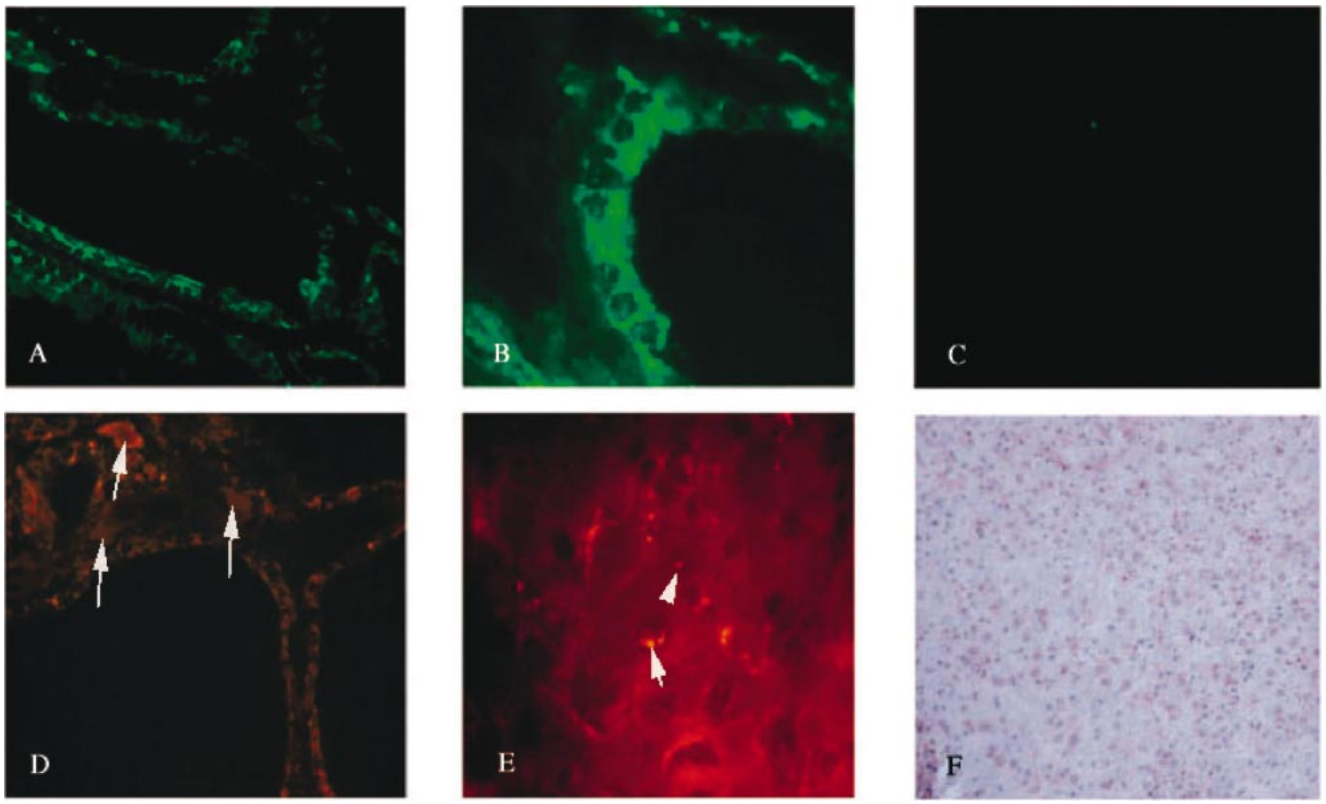

Fig 2. AlphaB-crystallin and Hsp27-1 immunofluorescence staining of goiter and anaplastic thyroid carcinoma (ATC) tissue. Cryosections (4 μm) of goiter- and ATC-derived tissue were stained with anti–alphaB-crystallin antibody (Ab) and anti-Hsp27-1 monoclonal antibody using the immunofluorescence technique. (A) Considerable alphaB-crystallin–specific immunofluorescence signals were detected in goiter-derived tissue sections (magnification 200×). (B) All thyrocytes exhibited a cytoplasmic alphaB-crystallin immunostaining, which accumulated in juxtaposition to the nucleus (arrows; magnification 800×). (C) AlphaB-crystallin was completely absent in 1 of the tested ATC specimens (magnification 800×). (D) Benign thyrocytes exhibited considerable cytoplasmic Hsp27-1 immunostaining (magnification 200×). Hsp27-1 immunoreactivity was infrequently detected in the follicular colloid to variable extent (arrow). (E) A similar extent of Hsp27-1 immunostaining was detected in ATC-derived tissue sections. Interestingly, some of the anaplastic thyrocytes exhibited a nuclear, speckled Hsp27-1 staining (arrows) in addition to the mainly cytoplasmic staining pattern (magnification 1000×). (F) The characteristic histopathological appearance of ATCs is demonstrated by hematoxylin-eosin (HE) staining (magnification 400×).

exhibited a speckled, nuclear Hsp27-1–staining pattern in addition to the cytoplasmic immunostaining observed in the other tissue specimens. Hsp27-1–specific colloidal immunostaining was found infrequently and to a variable extent in the tested goiters ($n = 7$, Fig 2D). In contrast, alphaB-crystallin–specific immunostaining was absent in the colloid of all tested goiters. The characteristic ATC morphology was confirmed by hematoxylin-eosin (HE) staining of the tested tumor samples (Fig 2F).

Three different fragments of each individual tumor were investigated. Five sections were stained for each tumor type from each block. Representative images are shown. Staining specificity was confirmed by antibody preadsorption as described above.

Exclusion of relevant ATC-specific alphaB-crystallin gene (CRYAB) and promoter sequence variations

Tumor-specific alterations of the CRYAB gene or of its promoter sequence might represent a potential cause for the consistent reduction of alphaB-crystallin expression in ATC tissue. Therefore, somatic DNA derived from ATC ($n = 3$) and goiter tissue ($n = 3$) was subjected to CRYAB gene–specific Southern blot and alphaB-crystallin promoter sequence analysis. However, neither the Southern blot using restriction enzyme digests with Taq1, Msp1, and EcoR1/BamH1, respectively, nor the promoter sequence analysis revealed any tumor-specific variations (data not shown).

It has to be stressed that the biological relevance of the 712-bp promoter sequence, which was used for this and the subsequent analysis, was confirmed in the course of luciferase reporter assays (Fig 3). Transient transfection of Cos cells with the 712-bp alphaB-crystallin-promoter luciferase-reporter plasmid and subsequent exposition of these cells to thermal stress (40°C, 4 hours) resulted in a significant ($P < 0.002$) increase of the transcriptional activity when compared with basal tissue culture conditions (37°C). In contrast, hyperglycemic stress had no effect on the promoter activity (data not shown). In addi-

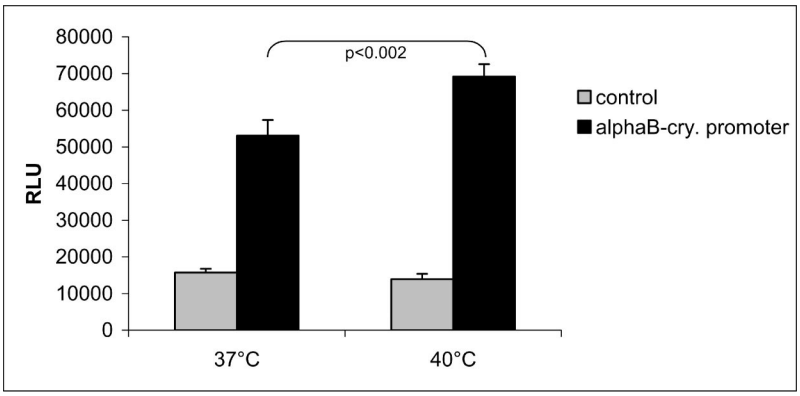

Fig 3. Heat shock transcription induction by the analyzed 712-bp promoter fragment of alphaB-crystallin. Cos cells endogenously expressing alphaB-crystallin were transiently transfected with a luciferase reporter plasmid containing the 712-bp fragment, which was used in all the promoter analysis. Luciferase assays were performed 48 hours after transfection in a Berthold luminometer. Heat shock exposition for 4 hours at 40°C resulted in a significant ($P < 0.002$) transcription induction when compared with basal culture conditions (37°C).

tion, the ATC cell line C-643 (Heldin et al 1988) was transiently transfected with the 712-bp alphaB-crystallin-promoter luciferase-reporter plasmid. Reflecting our immunoblot and quantitative RT-PCR data, no transcriptional activity driven by the 712-bp alphaB-crystallin promoter fragment was detectable (data not shown).

Effect of CpG island methylation status on alphaB-crystallin expression

CpG island methylation is a recently described mechanism of tumor-specific gene silencing (Herman and Baylin 2003). Within the CRYAB gene, numerous CpG biguanides exist, with highest abundance within the promoter region. Thus, CpG island methylation might represent one of the underlying causes of alphaB-crystallin expression suppression observed in ATCs. The CRYAB gene including the 712-bp promoter region contains 6 cutting sites (CCGG, Fig 4A, upper panel) specifically recognized by the restriction enzymes *Hpa*II (methylation sensitve—ms) and the isoschizomer *Msp*I (methylation insensitive—mi). Differential methylation of CCGG sites would result in a restriction fragment length polymorphism (RFLP) using both enzymes in parallel Southern blot analysis. Consequently, we performed comparative restriction enzyme digests of ATC- and goiter-derived tissue, using the isoschizomers *Hpa*II and *Msp*I. Subsequent Southern blotting using probes specific for the coding part of the CRYAB gene (Fig 4B, upper panel) and specific for the 712-bp promoter region (Fig 4B, lower panel), respectively, was performed. Using the first probe, interindividual but not ATC-specific variations of detectable CpG island methylation (Fig 4B, upper panel; goiter 2, ATC1 vs goiter 1, 2, ATC2, 3) were revealed. When the promoter-specific probe was used, CpG island methylation of *Hpa*II or *Msp*I cutting sites with subsequent variation in the *Hpa*II-specific RFLP pattern was present exclusively in ATC3 (Fig 4B, lower panel). Bioinformatic alphaB-crystallin promoter analysis indicated that the 2240-bp restriction fragment (Fig 4A,B, lower panel, marked by an asterisk), which occurred when ATC3 was the subject of testing, resulted from methylation of all *Msp*I or *Hpa*II cutting sites within the 712-bp promoter region and from methylation of additional *Msp*I or *Hpa*II cutting sites located upstream of this promoter fragment (Fig 4A). Thus, whereas CpG island methylation of CRYAB gene sequences downstream of the promoter region was detectable in benign and malignant thyroid tissue, methylation within the alphaB-crystallin promoter region was found only in one of the ATCs (ATC 3).

To further analyze the effect of CpG island methylation on CRYAB gene silencing, C-643 cells, which are characterized by complete absence of alphaB-crystallin expression, were treated with the demethylating agent 5-azacytidine for 24 hours and for 72 hours, respectively. However, consecutive alphaB-crystallin immunoblotting (data not shown) and quantitative RT-PCR (Fig 1B) revealed persistence of CRYAB gene silencing after 5-azacytidine treatment.

Identification of differences between the transcription factor expression pattern of ATC and goiter tissue

Promoter methylation was detectable only in one of the tested ATCs, and the demethylating agent 5-azacytidine had no influence on alphaB-crystallin expression in C-643 cells. Thus, tumor-specific transcription factor expression patterns might be the main cause for CRYAB gene expression regulation. To address this point, we primarily entered the 712-bp promoter sequence into a mammalian DNA motif search program. Using a cutoff value of 85, we found 28 different motifs with a high score (>85) for specific binding sites of well-defined transcription factors within the 712–bp fragment of the CRYAB gene promoter

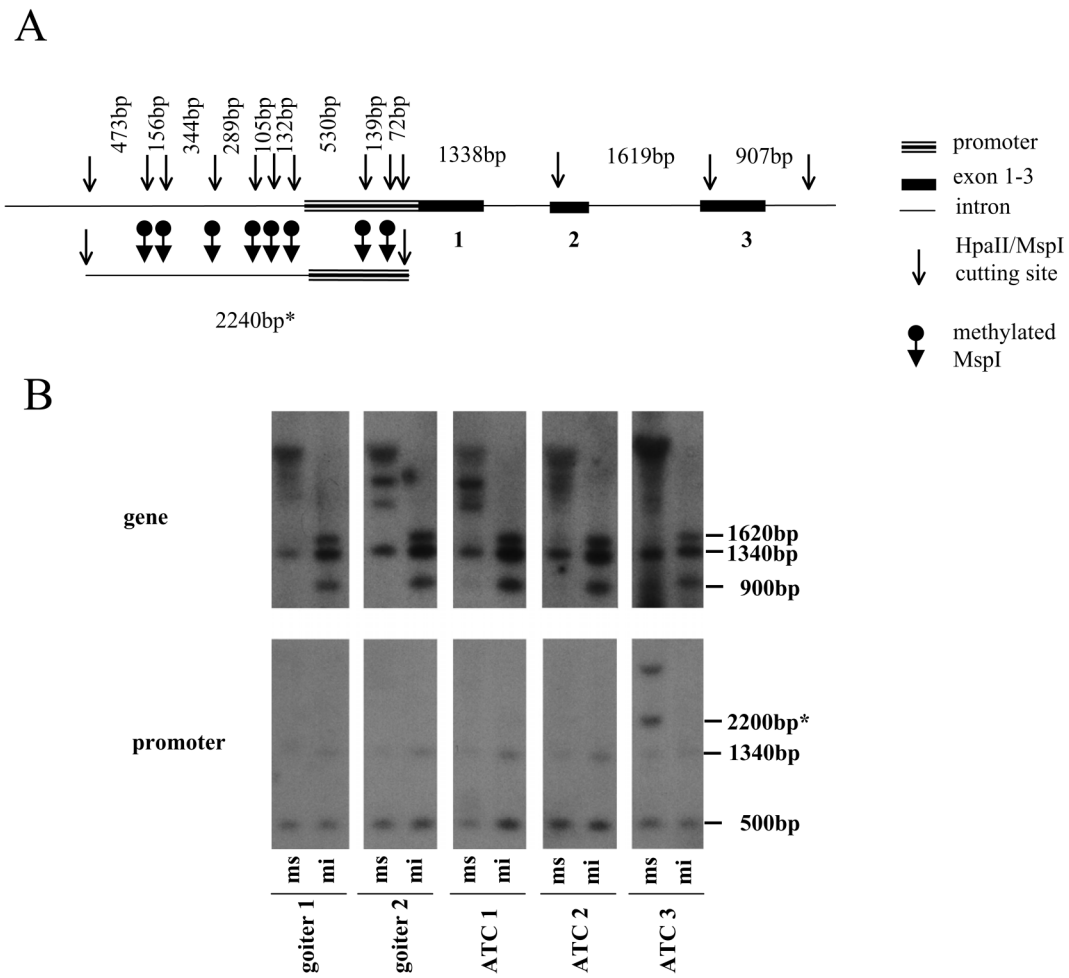

Fig 4. Evaluation of the CpG island methylation status within the CRYAB gene or promoter sequence in benign and malignant thyroid tissue. (A) Within the CRYAB gene (including the 712-bp promoter element, exons 1–3, and interposed intronic sequences), 6 restriction sites (CCGG) specifically recognized by the isoschizomers *Msp*I and *Hpa*II exist. Upstream of the 712-bp fragment of the promoter, 7 additional restriction sites are located. These fragments are only observed by the promoter-specific probe when still connected with the downstream part of the promoter (712 bp) after *Hpa*II digest. (B) Using these restriction enzymes (*Msp*I = methylation insensitive—mi; *Hpa*II = methylation sensitive—ms), Southern blot analysis was performed. When ^{32}P-labeled probes consisting of the coding region of the CRYAB gene were used (upper panel), variations of the banding pattern because of CpG island methylation within the gene were present in all the tested samples. However, we were not able to identify a tumor-specific banding pattern. In contrast, when the promoter-specific, ^{32}P-labeled probe was used (lower panel), a methlyation-induced restriction fragment length polymorphism was found exclusively in one of the tested anaplastic thyroid carcinomas (ATC3). This ATC3-specific *Hpa*II banding pattern can only be explained by methylation of 6 potential cutting sites located upstream of the 712-bp promoter fragment. Depicted is 1 experiment out of 2.

(Fig 5; Table 1). Subsequently, we compared the gene expression patterns of ATC1, ATC2, and goiters (n = 2) by a human genome wide expression screening and focused on transcription factors involved in CRYAB gene expression regulation. Remarkable expression regulation of numerous alphaB-crystallin promoter interaction partners was revealed (Fig 6). Most strikingly, the transcription factor TFCP2L1 was markedly downregulated in ATC tissue when compared with benign goiter–derived tissue. In addition, the P300/CBP–associated factor (1.08 in goiter 1 and 2.25 in goiter 2 vs −0.14 in ATC1), p300 (goiter 1: 0.74 and goiter 2: 1.4 vs −0.61 in ATC1), and MZF1-binding zinc finger protein (goiter 1: 2.46 and goiter 2: 2.56 vs −0.09 in ATC1) were found to be downregulated in ATC1. GATA3 was upregulated in ATC1 when compared with goiter-derived tissue (goiter 1: −2.88 and goiter 2: −3.67 vs −1.05 in ATC1). This transcription factor was also analyzed using quantitative RT-PCR, which was performed for array data validation (data not shown). However, expression of this factor did not correlate with alphaB-crystallin expression in the tested samples. Interestingly, some of the transcription factors exhibited concordant regulation in both ATCs (eg, TFCP2L1, CRSP2, TCF11, and MZF1), whereas others were characterized by discordant regulation (eg, C/EBP beta and Lmo2).

In line with the less intense transcription regulation of

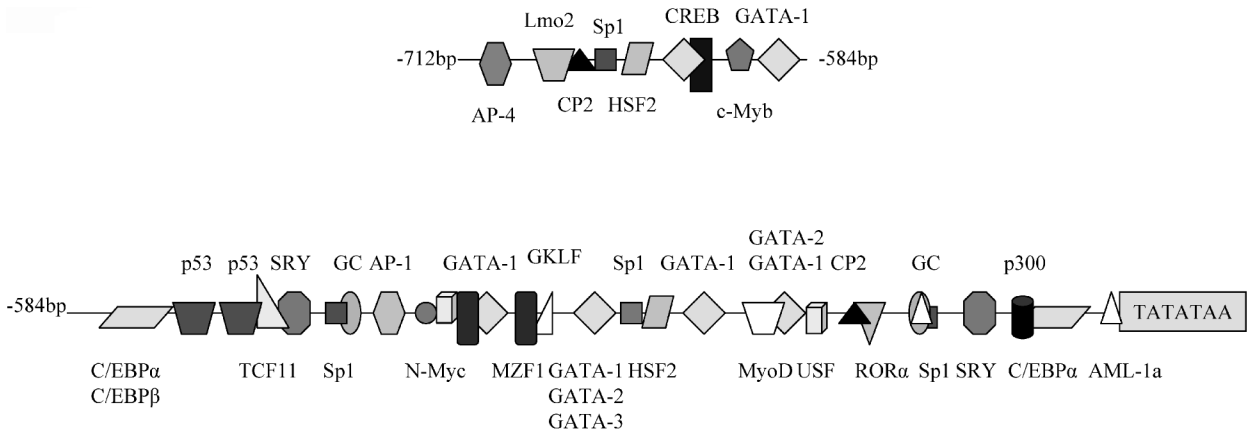

Fig 5. Bioinformatic analysis of the CRYAB gene promoter. Bioinformatic analysis of the CRYAB gene promoter fragment spanning 712 bp upstream of the transcription start site was performed. Identified responsive elements are depicted. Each transcription factor responsive element is represented by an individual symbol in the correct relative location to the TATA box.

Table 1 Comparison of the alphaB-crystallin promoter with the Hsp27-1 promoter with respect to their responsive elements

AlphaB-crystallin	Hsp27-1
AML-1a	**AML-1a**
AP-1 (2×)	
AP 4	
C/EBP (2×)	**C/EBP**
C/EBPalpha	
C/EBPbeta	**C/EPBbeta**
CdxA (2×)	**CdxA (2×)**
c-Myb	
CP2	**CP2**
CREB	
GATA-1	**GATA-1 (3×)**
GATA-2	**GATA-2 (3×)**
GATA-3	**GATA-3 (3×)**
GC	**GC**
GKLF	
HSF 1	**HSF 1**
HSF 2	**HSF 2**
Lmo2	
MyoD	
MZF1 (2×)	**MZF 1**
	Nkx-2.5
N-Myc	
P300	**P300**
P53	**P53**
RORalpha 1	
	RREB-1
Sp 1 (2×)	**Sp 1 (2×)**
SRY	**SRY**
TCF 11	
USF (2×)	**USF**
	v-Myb
	ZID

Bioinformatic analysis of alphaB-crystallin and the Hsp27-1 promoter fragments (712 bp upstream of the transcription start site) revealed considerable similarities in the constitution of both promoter elements. Responsive elements found within both promoters are given in bold letters. Remarkably, we also identified distinct responsive elements, which were present exclusively either within the Hsp27-1 promoter (eg, Nkx-2.5, RREB-1) or within the alphaB-crystallin promoter (eg, AP-1, c-Myb, CREB).

alphaB-crystallin in ATC2 (Fig 1B), variations between ATC1 and ATC2 with respect to the expression regulation of distinct transcription factors were observed. In ATC2, SP1, MyoD, and GKLF were upregulated and TCF11 and SRY were downregulated when compared with ATC1.

Identification of differences in the constitution of the alphaB-crystallin gene (CRYAB) and the Hsp27-1 gene (HSPB1) promoter

The differential expression of alpha-crystallin and Hsp27-1, despite a considerable degree of sequence homology, might be because of variations in their promoter sequences. Consequently, we compared the CRYAB and HSPB1 promoter regions with respect to their promoter element constitution. In analogy to alphaB-crystallin (see above), we entered the promoter sequences (712 bp upstream from the transcription start site) of HSPB1 into a mammalian DNA motif search program (cutoff value: 85). We found 21 different motifs with high score (>85) for specific binding sites of well-defined transcription factors within the HSPB1 promoter. There exists a high degree of similarity between the HSPB1 and CRYAB promoter regions (Table 1). Both contained HSF1 and HSF2 binding sites as characteristic attributes of heat-inducible proteins. However, the CRYAB gene promoter exhibited a more complex structure when compared with that of the HSPB1. This is exemplified by the presence of specific binding sites for AP1, AP4, C/EBPalpha, CREB, GKLF, Lmo2, MyoD, N-Myc, and RORalpha1, which were not present within the HSPB1 promoter. The responsive elements for Nkx-2.5, RREB-1, v-Myb, and ZID were found exclusively within the HSPB1 promoter. Some of the responsive elements were found repetitively within the 712-bp promoter fragments, eg, C/EBP, MZF, Sp1, USF, AP1 (CRYAB), GATA1–3 (HSPB1). Because of the identified

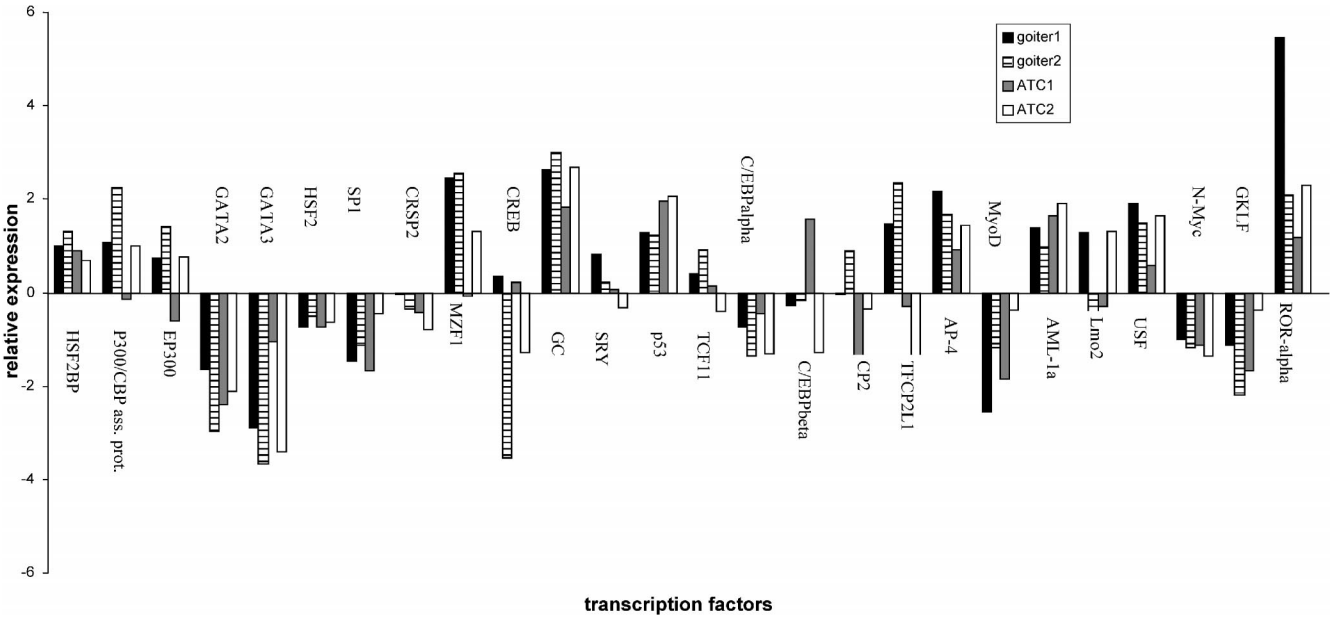

Fig 6. Comparison of alphaB-crystallin–specific transcription factor expression between goiter tissue and anaplastic thyroid carcinomas (ATC) tissue. After comparative gene array screening (goiter samples 1 and 2 vs ATC 1 and 2), we focused on expression regulation of alphaB-crystallin–specific transcription factors. The identified transcription factors and their relative expression are shown. Relative expression intensity was obtained by comparison of individual signals with reference ribonucleic acid provided by the manufacturer.

differences within the promoter regions, differential expression of both proteins, despite their high degree of sequence homology, seems plausible.

The CRYAB gene promoter interacting transcription factor TFCP2L1 is consistently downregulated in ATC-derived tissue

We further sought to identify a transcription factor influencing only the expression of the CRYAB gene but not that of HSPB1 gene. Although the TFCP2L1 corresponding promoter element CP2 is present within both the CRYAB gene and HSPB1 gene promoter (Table 1), earlier investigations revealed specific transcription regulation of alphaA-crystallin by CP2-interacting factors (Murata et al 1998). TFCP2L1 exhibited marked and concordant ATC-specific downregulation in the gene array screening. It is a member of the CP2 family of transcription factors, which are known for their transcription-inducing ability (Huang and Miller 2000). Therefore, TFCP2L1 was selected as a candidate transcription factor being mainly responsible for the ATC-specific CRYAB gene regulation and was subjected to further analysis. Confirming and extending our gene array results, quantitative RT-PCR revealed marked and consistent decrease of TFCP2L1 expression in ATC-derived tissues ($n = 6$) and in C-643 cells (Fig 7). Most importantly, the TFCP2L1 expression paralleled that of alphaB-crystallin in a tissue-specific manner.

DISCUSSION

In this study, we reveal marked downregulation of alphaB-crystallin in ATC tissue, which is in contrast to consistent Hsp27-1 expression in all the tested thyroid tissues. As one of the main potential mechanisms, we identified ATC-specific downregulation of the alphaB-crystallin promoter–interacting transcription factor TFCP2L1.

Involvement of heat shock proteins in tumor development and tumor cell survival because of cell-protective effects is a well-described phenomenon (Garrido et al 2003). Numerous epithelial tumors exhibited alphaB-crystallin expression, and alphaB-crystallin was even discussed as potential tumor marker (Pinder et al 1994; Chelouche-Lev et al 2004). In this context, earlier observations of strong expression of p29, which is used synonymously to Hsp27-1 in papillary thyroid carcinomas, and its correlation with distinct clinical attributes seems of special interest (Akslen and Varhaug 1995). Furthermore, ATCs are highly dedifferentiated and often exhibit strong variations in their protein expression pattern (Miura et al 2003; Segev et al 2003). Therefore, the consistent downregulation of alphaB-crystallin in all the tested ATC samples was surprising and might indicate a potential role of this protein as differentiation marker in thyroid tissues. In this respect, we want to stress that CRYAB gene silencing was similarly observed in a dedifferentiated medullary thyroid carcinoma as well as in a highly malignant

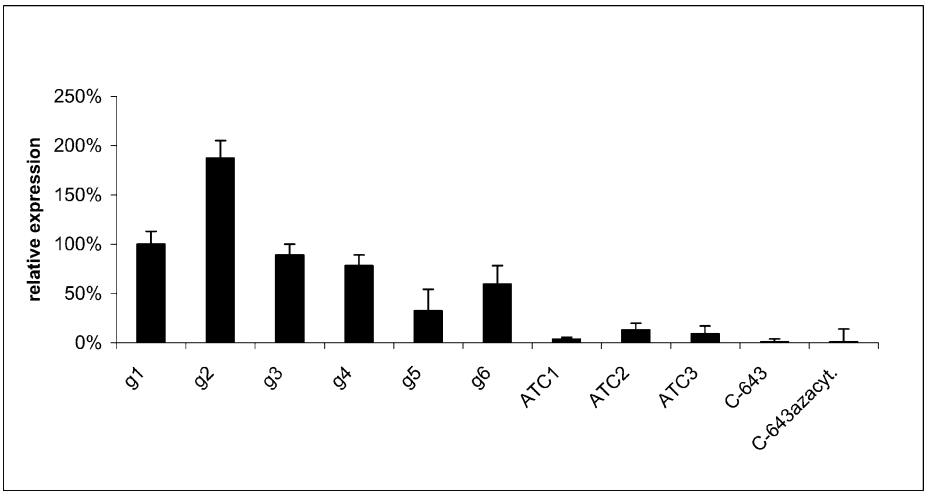

Fig 7. The CRYAB gene promoter interacting transcription inducer TFCP2L1 is downregulated in anaplastic thyroid tissue (ATC). TFCP2L1 was chosen for further expression quantification using quantitative RT-PCR of goiter- and ATC-derived tissue. Whereas TFCP2L1 was considerably expressed in all the tested goiter tissues (g1–g6), it was only marginally detectable in ATC-derived samples (ATC1–ATC3) and in C-643 cells. Pretreatment of C-643 cells with 5-azacytidine did not result in changes of the TFCP2L1 expression. All experiments were performed in duplicates, depicted is the extent of TFCP2L1 expression relative to TFCPL1 expression in goiter 1.

ovarian carcinoma (data not shown). Thus, CRYAB gene silencing might occur at the end of a stepwise dedifferentiation process, which seems not to be restricted to the thyroid gland. AlphaB-crystallin downregulation probably results in a decreased resistance against oxidative stress, finally leading to the high extent of chromosomal damage characteristically observed in ATCs (Zedenius et al 1996; Miura et al 2003; Wiseman et al 2003).

Hsp27-1 exhibits a considerable degree of sequence homology to alphaB-crystallin. In addition, for both proteins, similar intracellular functions are suspected, eg, both proteins inhibit tumor necrosis factor alpha–induced cell death (Mehlen et al 1996). Despite these similarities, alphaB-crystallin and Hsp27-1 exert their functions at least partly by divergent mechanisms (Kamradt et al 2001). This seems to be reflected by the intranuclear presence of Hsp27-1, which was not detectable for alphaB-crystallin. Thus, the differential expression of both proteins in ATCs is plausible and seems to be because of alphaB-crystallin–specific and Hsp27-1–specific promoter variations and gene-specific transcription factors.

Gene deletions or gene rearrangements are potential reasons for tumor-specific protein expression. Moreover, methylation of CpG islands within promoter regions of distinct genes has been identified as an epigenetic mechanism resulting in tumor-specific gene silencing (Herman and Baylin 2003). According to our data, neither of these mechanisms seems to be responsible for ATC-specific CRYAB gene silencing. However, we identify tumor-specific transcription factor expression patterns, which were consistently characterized by ATC-specific downregulation of TFCP2L1. Although this protein belongs to the CP2 family, which occurs ubiquitously in human tissues, members of this family of highly conserved transcription factors are known to be responsible for tissue-specific gene expression (Huang and Miller 2000; Rodda et al 2001). Most interestingly, CP2 family members have been demonstrated to specifically regulate alphaA-crystallin expression (Murata et al 1998). Thus, downregulation of TFCP2L1 seems to be one of the main mechanisms contributing to an interplay of transcription factors finally leading to CRYAB gene silencing.

We want to stress that, because of the small sample size, we do not intend to identify an ATC-specific transcription factor expression pattern. However, from our point of view, the presented data leave no doubt of CRYAB gene silencing in rapidly growing, dedifferentiated ATCs. The main underlying mechanism seems to be a tumor-specific transcription factor expression pattern, which is most prominently characterized by downregulation of the transcription factor TFCP2L1. Furthermore, CRYAB gene promoter methylation seems to be present in distinct tumors but its biological relevance has to be left open. The divergent expression regulation of Hsp27-1 and alphaB-crystallin supports the notion of biological differences between both small heat shock proteins, which has to be considered in future functional analysis.

ACKNOWLEDGMENTS

I.M. was a recipient of the Ernst Mach Scholarship of the Austrian Exchange Service. We want to thank Rita Lang for technical support and Prof Dr Georg Brabant for providing the C-643 cell line.

REFERENCES

Akslen LA, Varhaug JE. 1995. Oncoproteins and tumor progression in papillary thyroid carcinoma: presence of epidermal growth factor receptor, c-erbB-2 protein, estrogen receptor related protein, p21-ras protein, and proliferation indicators in relation to tumor recurrences and patient survival. *Cancer* 76: 1643–1654.

Bluhm WF, Martin JL, Mestril R, Dillmann WH. 1998. Specific heat shock proteins protect microtubules during simulated ischemia in cardiac myocytes. *Am J Physiol* 275: H2243–H2249.

Chelouche-Lev D, Kluger HM, Berger AJ, Rimm DL, Price JE. 2004. AlphaB-crystallin as a marker of lymph node involvement in breast carcinoma. *Cancer* 100: 2543–2548.

Dasgupta S, Hohman TC, Carper D. 1992. Hypertonic stress induces alpha B-crystallin expression. *Exp Eye Res* 54: 461–470.

Derham BK, Harding JJ. 1999. Alpha-crystallin as a molecular chaperone. *Prog Retin Eye Res* 18: 463–509.

Dubin RA, Ally AH, Chung S, Piatigorsky J. 1990. Human alpha B-crystallin gene and preferential promoter function in lens. *Genomics* 7: 594–601.

Dubin RA, Wawrousek EF, Piatigorsky J. 1989. Expression of the murine alpha B-crystallin gene is not restricted to the lens. *Mol Cell Biol* 9: 1083–1091.

Garrido C, Gurbuxani S, Ravagnan L, Kroemer G. 2001. Heat shock proteins: endogenous modulators of apoptotic cell death. *Biochem Biophys Res Commun* 286: 433–442.

Garrido C, Schmitt E, Cande C, Vahsen N, Parcellier A, Kroemer G. 2003. HSP27 and HSP70: potentially oncogenic apoptosis inhibitors. *Cell Cycle* 2: 579–584.

Golenhofen N, Ness W, Koob R, Htun P, Schaper W, Drenckhahn D. 1998. Ischemia-induced phosphorylation and translocation of stress protein alpha B-crystallin to Z lines of myocardium. *Am J Physiol* 274: H1457–H1464.

Groenen PJ, Merck KB, de Jong WW, Bloemendal H. 1994. Structure and modifications of the junior chaperone alpha-crystallin. From lens transparency to molecular pathology. *Eur J Biochem* 225: 1–19.

Heldin NE, Gustavsson B, Claesson-Welsh L, Hammacher A, Mark J, Heldin CH, Westermark B. 1988. Aberrant expression of receptors for platelet-derived growth factor in an anaplastic thyroid carcinoma cell line. *Proc Natl Acad Sci U S A* 85: 9302–9306.

Herman JG, Baylin SB. 2003. Gene silencing in cancer in association with promoter hypermethylation. *N Engl J Med* 349: 2042–2054.

Hickey E, Brandon SE, Potter R, Stein G, Stein J, Weber LA. 1986. Sequence and organization of genes encoding the human 27 kDa heat shock protein. *Nucleic Acids Res* 14: 4127–4145.

Horwitz J. 2003. Alpha-crystallin. *Exp Eye Res* 76: 145–153.

Huang N, Miller WL. 2000. Cloning of factors related to HIV-inducible LBP proteins that regulate steroidogenic factor-1-independent human placental transcription of the cholesterol side-chain cleavage enzyme, P450scc. *J Biol Chem* 275: 2852–2858.

Iwaki T, Kume-Iwaki A, Goldman JE. 1990. Cellular distribution of alpha B-crystallin in non-lenticular tissues. *J Histochem Cytochem* 38: 31–39.

Kamradt MC, Chen F, Cryns VL. 2001. The small heat shock protein alpha B-crystallin negatively regulates cytochrome c- and caspase-8-dependent activation of caspase-3 by inhibiting its autoproteolytic maturation. *J Biol Chem* 276: 16059–16063.

Kamradt MC, Chen F, Sam S, Cryns VL. 2002. The small heat shock protein alpha B-crystallin negatively regulates apoptosis during myogenic differentiation by inhibiting caspase-3 activation. *J Biol Chem* 277: 38731–38736.

Kappe G, Franck E, Verschuure P, Boelens WC, Leunissen JA, de Jong WW. 2003. The human genome encodes 10 alpha-crystallin-related small heat shock proteins: HspB1–10. *Cell Stress Chaperones* 8: 53–61.

Kappe G, Verschuure P, Philipsen RL, Staalduinen AA, Van de Boogaart P, Boelens WC, De Jong WW. 2001. Characterization of two novel human small heat shock proteins: protein kinase-related HspB8 and testis-specific HspB9. *Biochim Biophys Acta* 1520: 1–6.

Klemenz R, Andres AC, Frohli E, Schafer R, Aoyama A. 1993. Expression of the murine small heat shock proteins hsp 25 and alpha B crystallin in the absence of stress. *J Cell Biol* 120: 639–645.

Liang P, MacRae TH. 1997. Molecular chaperones and the cytoskeleton. *J Cell Sci* 110(Pt 13): 1431–1440.

Mehlen P, Kretz-Remy C, Preville X, Arrigo AP. 1996. Human hsp27, Drosophila hsp27 and human alphaB-crystallin expression-mediated increase in glutathione is essential for the protective activity of these proteins against TNFalpha-induced cell death. *EMBO J* 15: 2695–2706.

Mitton KP, Tumminia SJ, Arora J, Zelenka P, Epstein DL, Russell P. 1997. Transient loss of alphaB-crystallin: an early cellular response to mechanical stretch. *Biochem Biophys Res Commun* 235: 69–73.

Miura D, Wada N, Chin K, Magrane GG, Wong M, Duh QY, Clark OH. 2003. Anaplastic thyroid cancer: cytogenetic patterns by comparative genomic hybridization. *Thyroid* 13: 283–290.

Muchowski PJ, Valdez MM, Clark JI. 1999. AlphaB-crystallin selectively targets intermediate filament proteins during thermal stress. *Investig Ophthalmol Vis Sci* 40: 951–958.

Murata T, Nitta M, Yasuda K. 1998. Transcription factor CP2 is essential for lens-specific expression of the chicken alphaA-crystallin gene. *Genes Cells* 3: 443–457.

Neuhofer W, Fraek ML, Beck FX. 2005. Differential expression of heat shock protein 27 and 70 in renal papillary collecting duct and interstitial cells—implications for urea resistance. *J Physiol* In press.

Parcellier A, Schmitt E, Brunet M, Hammann A, Solary E, Garrido C. 2005. Small heat shock proteins HSP27 and alphaB-crystallin: cytoprotective and oncogenic functions. *Antioxid Redox Signal* 7: 404–413.

Perou CM, Sorlie T, Eisen MB, et al. 2000. Molecular portraits of human breast tumours. *Nature* 406: 747–752.

Pinder SE, Balsitis M, Ellis IO, Landon M, Mayer RJ, Lowe J. 1994. The expression of alpha B-crystallin in epithelial tumours: a useful tumour marker? *J Pathol* 174: 209–215.

Rodda S, Sharma S, Scherer M, Chapman G, Rathjen P. 2001. CRTR-1, a developmentally regulated transcriptional repressor related to the CP2 family of transcription factors. *J Biol Chem* 276: 3324–3332.

Segev DL, Umbricht C, Zeiger MA. 2003. Molecular pathogenesis of thyroid cancer. *Surg Oncol* 12: 69–90.

Sherlock G, Hernandez-Boussard T, Kasarskis A, et al. 2001. The stanford microarray database. *Nucleic Acids Res* 29: 152–155.

Tremolada L, Magni F, Valsecchi C, et al. 2005. Characterization of heat shock protein 27 phosphorylation sites in renal cell carcinoma. *Proteomics* 5: 788–795.

Wang K, Spector A. 1996. Alpha-crystallin stabilizes actin filaments and prevents cytochalasin-induced depolymerization in a phosphorylation-dependent manner. *Eur J Biochem* 242: 56–66.

Webster KA. 2003. Serine phosphorylation and suppression of apoptosis by the small heat shock protein alphaB-crystallin. *Circ Res* 92: 130–132.

White BG, Williams SJ, Highmore K, Macphee DJ. 2005. Small heat shock protein 27 (Hsp27) expression is highly induced in rat

myometrium during late pregnancy and labour. *Reproduction* 129: 115–126.

Whitlock NA, Agarwal N, Ma JX, Crosson CE. 2005a. Hsp27 upregulation by HIF-1 signaling offers protection against retinal ischemia in rats. *Investig Ophthalmol Vis Sci* 46: 1092–1098.

Whitlock NA, Lindsey K, Agarwal N, Crosson CE, Ma JX. 2005b. Heat shock protein 27 delays Ca2+-induced cell death in a caspase-dependent and -independent manner in rat retinal ganglion cells. *Investig Ophthalmol Vis Sci* 46: 1085–1091.

Wiseman SM, Loree TR, Rigual NR, Hicks WL Jr, Douglas WG, Anderson GR, Stoler DL. 2003. Anaplastic transformation of thyroid cancer: review of clinical, pathologic, and molecular evidence provides new insights into disease biology and future therapy. *Head Neck* 25: 662–670.

Zedenius J, Wallin G, Svensson A, Bovee J, Hoog A, Backdahl M, Larsson C. 1996. Deletions of the long arm of chromosome 10 in progression of follicular thyroid tumors. *Hum Genet* 97: 299–303.

Zierhut B, Mechtler K, Gartner W, Daneva T, Base W, Weissel M, Niederle B, Wagner L. 2004. Heat shock protein 70 (Hsp70) subtype expression in neuroendocrine tissue and identification of a neuroendocrine tumour-specific Hsp70 truncation. *Endocr Relat Cancer* 11: 377–389.